AIAA JOURNAL
Vol. 44, No. 8, August 2006

Numerical Simulation and Reduced-Order Modeling of Airfoil Gust Response

Avi Zaide* and Daniella Raveh†
Technion—Israel Institute of Technology, 32000 Haifa, Israel

DOI: 10.2514/1.16995

Computational fluid dynamics (CFD) based simulations, along with parametric and nonparametric reduced-order models for gust responses are presented. A CFD code is enhanced to simulate responses of an airfoil to arbitrary-shaped gust inputs. Time-domain autoregressive-moving-average models are identified based on CFD responses to random gust excitations, using system-identification methods. Responses to discrete gusts of various shapes, amplitudes, and gradient lengths are computed via the reduced-order models and compared to responses simulated directly by the CFD code. The reduced-order models predict the lift and pitching moment histories accurately throughout the subsonic and transonic regimes. They offer significant savings in computational resources compared to the full CFD simulation, because only one CFD run is required for reduced-order model identification, from which responses to arbitrary-shaped gusts can be rapidly estimated. The combination of reduced-order models and full CFD simulation offers a computationally efficient tool set of various-fidelity time-domain models for gust responses. The reduced-order model can be used for rapid tuned-gust analyses, and the critical cases can be simulated with a full CFD run, providing pressure distribution for airframe structural design.

Nomenclature

a	=	speed of sound
a_i	=	ARMA model coefficient
b	=	semichord length
b_i	=	ARMA model coefficients
C_l	=	lift coefficient
c	=	chord length
f_s, f_{Nyq}	=	sampling frequency, Nyquist frequency
M	=	Mach number
N	=	number of iterations
n	=	discrete time
n_a, n_b	=	ARMA model order
s	=	nondimensional time
t	=	time
U, V, W	=	velocities in curvilinear coordinates
U_g	=	gust velocity
U_∞	=	far-field flow velocity
u, v, w	=	velocities in Cartesian coordinates
w_g	=	gust velocity
$w_{3/4c}$	=	velocity at three-quarter chord
$X(n)$	=	state vector of a state-space model
x, $\bar{x}$	=	length, nondimensional length
α_0	=	angle of attack
η	=	fit parameter
λ	=	advance ratio
ξ, η, ζ	=	CFD grid coordinates
$\xi_{x,y,z}$, $\eta_{x,y,z}$, $\zeta_{x,y,z}$	=	grid spatial derivatives
ξ_t, η_t, ζ_t	=	grid time metrics
ρ	=	flow density
$\phi(s)$	=	Wagner function
$\psi(s)$	=	Küssner function

Introduction

THE current study is the first phase in the development of models for the evaluation of the dynamic loads on an elastic aircraft in atmospheric gust, based on numerical simulations using a computational fluid dynamics (CFD) code. Aeroelastic gust response analysis requires an aerodynamic model of the unsteady forces that develop on the aircraft as it travels through atmospheric gust. Traditionally, two methods are used for discrete-gust (i.e., deterministic gust) aerodynamic loads, namely the time-domain and frequency-domain methods. The time-domain approach is based on the Wagner and Küssner functions that provide the analytical lift buildup in response to a step change in the angle of attack (AOA) and to a sharp-edge gust, respectively. The Wagner and Küssner functions are valid for incompressible flows, and closed-form approximations are available for compressible flows. These are used in convolution schemes to compute the response to an arbitrary-shaped gust excitation. The advantage of convolution models is that they readily provide the time history of the aerodynamic forces. Their shortcoming is that the Wagner and Küssner analytical functions and their compressible approximations are valid for a two-dimensional flat plate. A three-dimensional extension is possible by considering the lift per unit span to equal the two-dimensional flat-plate lift. However, this extension is only valid for straight and slender wings. Convolution models are also less suitable for use in aeroservoelastic (ASE) analysis, in which a control system is augmented, and which is typically performed using state-space models. Frequency-domain aerodynamics is used in conjunction with the frequency-domain formulation of the aeroelastic equation of motion in generalized coordinates. The gust velocity input is expressed as a combination of harmonic excitations of various reduced frequencies, and the gust generalized aerodynamic forces are computed using the generalized aerodynamic influence coefficient matrices (AICs) at these reduced frequencies. For time-response simulation, or for ASE analysis, a time-domain state-space gust response model can be extracted by rational function approximation [1,2] or other reduced-order modeling techniques [3]. However, this extraction is not straightforward [1,3].

This study aims at exploiting the currently available numerical CFD tools for gust response analyses. CFD codes are typically thought of as tools for nonlinear flows. In this study, however, it is suggested to exploit them for both the subsonic and transonic flow regimes, by using a combination of full CFD simulations and CFD-based reduced-order models (ROMs) that together offer time-domain models of various fidelity for gust responses.

The literature on CFD-based gust response analysis is recent and very limited. The major interest in CFD-based gust response analysis came from the helicopter community, mainly for blade-flow

Received 6 April 2005; revision received 1 December 2005; accepted for publication 29 January 2006.

*Graduate Student, Faculty of Aerospace Engineering.
†Senior Lecturer, Faculty of Aerospace Engineering. Member AIAA.

interactions. Parameswaran and Baeder [4], and Singh and Baeder [5,6] proposed the *field velocity* approach in which the velocity induced by the impulsive or gradual change in AOA, due to gust, is prescribed to the grid time metrics without moving the computational mesh. In these studies an unsteady Euler solver was enhanced to simulate the indicial response of an airfoil and a rectangular wing to a step change in the AOA and sharp-edge gust. Recently, Yang and Obayashi [7] addressed the dynamic response in vertical gust of a supersonic transport model. A direct coupling between the flow and structural dynamic equations of motion was applied, and a Navier–Stokes-based simulation of responses to discrete gust was performed. This study examined gust responses in simulations that involved 2 degrees of freedom in motion, in pitch and plunge, with and without the effect of elastic deformations.

These CFD-based gust studies lay the basic foundations and proof of concept for CFD-based gust response simulations. The major hindrance of CFD-based methods is the large computational time associated with each run. This is even more so in dynamic problems that require simulation over large times using small time steps. Each simulation is extremely computationally expensive, making such an approach impractical in the environment of production aircraft design. To take advantage of CFD methods in a computationally feasible manner, the current study proposes to explore reduced-order modeling of CFD-based time-domain unsteady aerodynamics.

The EZNSS [8] (elastic zonal Navier–Stokes simulation) CFD code is enhanced to simulate the time history of the aerodynamic response to arbitrary gust inputs. Lift responses of an airfoil to a step change in the AOA, and to a sharp-edge gust are computed and serve as convolution models. Validation is achieved by comparing the lift time history computed at various Mach numbers to the analytical Wagner and Küssner functions and their compressible closed-form approximations. Autoregressive-moving-average (ARMA) models are identified from a set of CFD input–output data. Gust responses for gust inputs of various shape, amplitude, and gradient length are estimated via the ROMs and compared to responses from full CFD simulations.

The ROMs proposed in the current study are all linearized, therefore the method could be applied with a potential code instead of the Euler code. The benefits of the use of CFD Euler/Navier–Stokes codes are twofold. First, it captures the nonlinear steady-state flow phenomena upon which linearization is made. Secondly, the same model can be used both for ROM generation and for a comprehensive nonlinear full simulation. The CFD-ROM approach offers a tool set of various-fidelity models for gust response analysis, in which the ROM can be used for rapid gust analysis and the full CFD simulation is used to analyze critical loading cases.

Mathematical Model

Following the formulation of [9], the indicial lift buildup (the circulatory part of the lift) in response to a step input of the AOA is expressed as

$$L = 2\pi\rho U_\infty^2 b\alpha_0\phi(s) \tag{1}$$

where ρ and U_∞ are the flow density and speed, respectively, b is the semichord length, α_0 is the angle of attack, s is the nondimensional time, namely the length in semichords traveled from the leading edge, $s = tU_\infty/b$, and $\phi(s)$ is the Wagner function approximated as

$$\phi(s) \cong 1 - 0.165e^{-0.0455s} - 0.335e^{-0.3s} \tag{2}$$

An arbitrary time-dependent angle of attack input acting on the airfoil can be described by the time-dependent velocities of its three-quarter chord point, as

$$w_{3/4c} = U_\infty\alpha_0(s) \qquad s > 0 \tag{3}$$

These, in turn, can be considered as superposition of velocity step inputs, and the lift response can then be computed by convolution, using the Wagner function, as

$$L = 2\pi\rho U_\infty b\left[w_{3/4c}(0)\phi(s) + \int_0^s \frac{\mathrm{d}w_{3/4c}(\sigma)}{\mathrm{d}\sigma}\phi(s-\sigma)\mathrm{d}\sigma\right] \tag{4}$$

Similarly, a sharp-edge gust encountered at the leading edge at $s = 0$ is expressed as

$$w_g = \begin{cases} w_g, & \bar{x} < -1 + s \\ 0, & \bar{x} > -1 + s \end{cases} \tag{5}$$

where $\bar{x}$, the nondimensional length, equals x/b. Figure 1 presents the sharp-edge gust front at the leading edge at $s = 0$. The lift due to the sharp-edge gust is provided by

$$L = 2\pi\rho U_\infty b w_g\psi(s) \tag{6}$$

in which $\psi(s)$ is approximated by

$$\psi(s) \cong 1 - 0.5e^{-0.13s} - 0.5e^{-s} \tag{7}$$

The lift buildup in response to an arbitrary-shaped gust input can be evaluated by convolution as

$$L = 2\pi\rho U_\infty b\left[w_g(0)\psi(s) + \int_0^s \frac{\mathrm{d}w_g(\sigma)}{\mathrm{d}\sigma}\psi(s-\sigma)\mathrm{d}\sigma\right] \tag{8}$$

Equations (1–8) outline the theory of airfoil response to step AOA and sharp-edge gust for incompressible flows. For compressible flows, these responses can be represented in an approximate exponential form as

$$\phi(s) = c_0 + c_1e^{-\beta_1 s} + c_2e^{-\beta_2 s} + c_3e^{-\beta_3 s} \tag{9}$$

The coefficients of Eq. (9), for both the step AOA and sharp-edge gust responses, are brought in Tables 6-1 and 6-2, in Chapter 6 of Ref. [9] (taken from Mazelsky and Drischler [10] for Mach numbers 0, 0.5, 0.6, and 0.7). This extension to the subsonic compressible domain has been practically used in the current study as the reference to responses computed via the CFD Euler analysis. Other closed-form solutions to the compressible responses are presented by Lomax [11] and by Leishman [12,13].

The first goal of this study is to numerically simulate a general gust input function with a CFD code, to validate the flow analysis by comparison of the step AOA and sharp-edge gust responses with their closed-form approximations [according to Eq. (9), also presented as Figs. 6-12(a) and 6-13 of [9]], and to study these responses in compressible and incompressible flows for various thickness airfoils. Then the response to an arbitrary AOA or gust excitation can be calculated either by convolution [following Eqs. (4) and (8)] or directly by numerical simulation, comparing the time histories of the responses. Provided that the CFD-simulated responses are linear or near linear, that is, provided that the combination of Mach number, airfoil shape, and gust-induced AOA does not result in strong shocks, convolution according to Eqs. (4) and (8) should predict the forces buildup accurately.

AOA and Gust Input Implementation within the CFD Code

Numerical simulation is performed with the in-house Euler/Navier–Stokes code EZNSS [8] that is a time-accurate implicit finite-difference code, employing the Beam and Warming algorithm. The AOA step input is introduced to the flowfield by prescribing to all of the grid points a vertical velocity of $U_\infty\alpha_0$, α_0 being the AOA magnitude, starting at $s = 0$. Similarly, a sharp-edge gust input is introduced by prescribing the gust vertical velocity, w_g to all grid

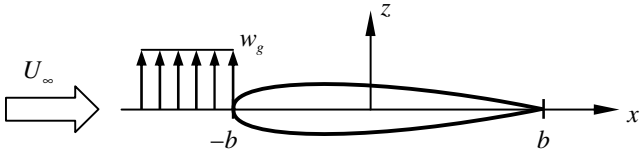

Fig. 1 Sharp-edge gust front at $s = 0$.

points with flow-direction coordinate $\bar{x}$ of $\bar{x} \leq -1 + s$.

Prescribing vertical gust velocities is done following the field velocity approach suggested by Parameswaran and Baeder [4], and Singh and Baeder [5,6]. In the formulation of the flowfield equations in curvilinear coordinates, as stated by Eq. (10), this is done by assigning the vertical velocities to the grid time metrics ξ_t, η_t, and ζ_t. In Eq. (10) the u, v, w and U, V, W terms are the velocities in the Cartesian and curvilinear coordinates, respectively. A complete account of the various terms of Eq. (10) is found in [14]. It should be noted that the gust vertical velocities are subscribed to the grid without actually moving the grid.

$$\begin{Bmatrix} U - \xi_t \\ V - \eta_t \\ W - \zeta_t \end{Bmatrix} = \begin{bmatrix} \xi_x & \xi_y & \xi_z \\ \eta_x & \eta_y & \eta_z \\ \zeta_x & \zeta_y & \zeta_z \end{bmatrix} \begin{Bmatrix} u \\ v \\ w \end{Bmatrix} \tag{10}$$

Parametric Modeling of Gust Response

Next we wish to identify a parametric model of the aerodynamic gust response. The advantage of a parametric model over a convolution model is that it is very computationally efficient, unlike the convolution model which requires considerable computation when evaluated over extended times. Moreover, when a control system is augmented, and the ASE system is represented by a time-domain state-space model, the aerodynamic parametric model can be directly integrated into the ASE formulation.

The aerodynamic gust response is modeled by an ARMA model that relates the aerodynamic lift coefficient (or possibly another aerodynamic response, for example, the pitching moment) to the gust input at the current and previous time steps, and to previous time-step values of the lift coefficient. The ARMA model assumes the following model structure:

$$\begin{aligned} C_l(n) = &-a_1 C_l(n-1) - a_2 C_l(n-2) - \cdots - a_{n_a} C_l(n-n_a) \\ &+ b_0 w_g(n) + b_1 w_g(n-1) + \cdots + b_{n_b} w_g(n-n_b) \end{aligned} \tag{11}$$

where $C_l(n)$ is the time-dependent lift coefficient, and $w_g(n)$ is the gust input, which is the value of the gust velocity at the leading edge at discrete time n. n_a and n_b are the model orders that are determined by the user, and $a_1 \cdots a_{n_a}$, b_0, $b_1 \cdots b_{n_b}$ are the model parameters to be estimated.

The first step in construction of an ARMA model is the selection of model orders n_a and n_b, which, in this case, state how much of the history of the lift and of the gust excitation needs to be accounted for, to get accurate representation of the unsteady aerodynamic gust response. To gain insight of the required order of the ARMA model, we note that the Küssner function of Eq. (7), can be written as an ARMA model of the order $n_a = 2$, $n_b = 1$, and its parameters a_1, a_2 and b_0 and b_1 can be calculated exactly for various values of discrete-time steps, Δs, as follows:

$$\begin{gathered} a_1 = -\frac{1.13\Delta s + 2}{0.13\Delta s^2 + 1.13\Delta s + 1}, \\ a_2 = \frac{1}{0.13\Delta s^2 + 1.13\Delta s + 1}, \qquad b_0 = \frac{0.13\Delta s^2 + 0.565\Delta s}{0.13\Delta s^2 + 1.13\Delta s + 1}, \\ b_1 = -\frac{0.565\Delta s}{0.13\Delta s^2 + 1.13\Delta s + 1} \end{gathered} \tag{12}$$

It is therefore decided to use a 2, 1 ARMA model for the lift response of Eq. (11). By doing so, it is also possible to compare the identified parameters a_1, a_2, b_0, and b_1 to the exact ones from Eq. (12), and gain an estimate on the accuracy of the identification process.

Next, a data set for the identification is generated. In this case, the identification data consist of the time histories of lift coefficients that develop in response to *random* gust input, computed in a CFD run. A complete discussion of the excitation signal is presented in the ARMA Model section. Model parameters are identified based on the identification data, such that they minimize the prediction error of Eq. (11) in a least square sense (see [15] for details on parameter identification). The accuracy of the model is estimated by computing responses to various input signals for which the exact response is known, in the case of this study from direct CFD simulation. A fit parameter is used to estimate the model accuracy, according to

$$\eta = \left(1 - \sqrt{\frac{\sum_{i=1}^{N} (C_{l_i} - \hat{C}_{l_i})^2}{\sum_{i=1}^{N} C_{l_i}^2}}\right) \tag{13}$$

where C_l and $\hat{C}_l$ are the vectors of exact (from CFD simulation) and estimated (from the ARMA model) lift coefficients, respectively. A value of 1 of the fit parameter indicates a perfect fit between the estimated and exact values.

The ARMA model can be converted straightforwardly into a state-space model. For example, the 2, 1 ARMA model of Eq. (11) can be expressed as the following state-space model:

$$\begin{cases} X(n) = \begin{bmatrix} -a_1 & -a_2 \\ 1 & 0 \end{bmatrix} X(n-1) + \begin{bmatrix} b_0 \\ (-\frac{b_1}{a_2}) \end{bmatrix} w_g(n) \\ C_l(n) = \begin{bmatrix} 1 & 0 \end{bmatrix} X(n) \end{cases} \tag{14}$$

where the model states are

$$\begin{cases} X_1(n) = C_l(n) \\ X_2(n) = C_l(n-1) \end{cases} \tag{15}$$

Numerical Application

Indicial responses and responses to sharp-edge gust were computed by the EZNSS code for the NACA0004, NACA0006, and NACA0012 airfoils. The *C*-type mesh consists of 399 grid points in the chordwise direction (ξ direction), along the wing and its wake, and 71 grid points along the direction normal to the wing surface (η direction). The grid extends 13 chords behind the wing's trailing edge. The steady-state flowfield at zero-degrees AOA is first evaluated and serves as the starting condition for all the following simulations. All the following analyses are based on a nondimensional time step of 0.01. It should be noted that it is the CFD code convention to use c/a and c as the time and length units, for nondimensionalization. This is in contrast to the analytical formulation of Eqs. (1–9), which uses b/U_∞ and b as the time and length units.

Figure 2 presents responses to a step AOA of 2 deg, at various Mach numbers. The responses are normalized by the steady-state

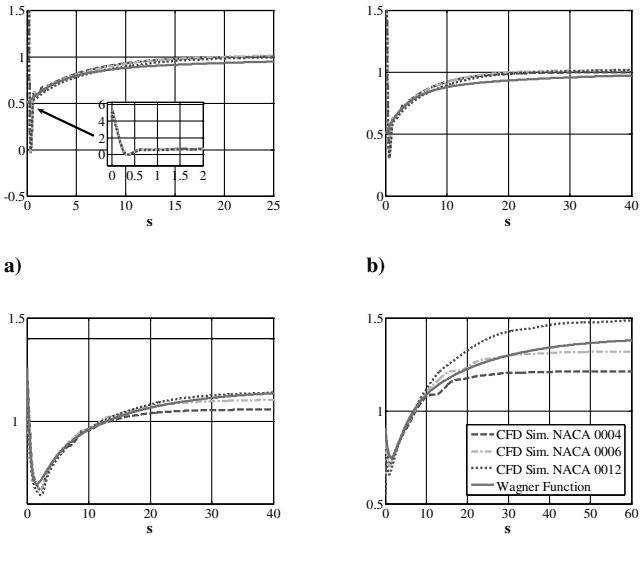

Fig. 2 Normalized indicial response to a step AOA. Mach 0.11 a), Mach 0.2 b), Mach 0.5 c), Mach 0.7 d).

value of the incompressible lift coefficients, which are computed from steady CFD runs of the various airfoils at Mach 0.11. The CFD responses are compared to the incompressible Wagner function at Mach numbers 0.11 and 0.2, and to the compressible closed-form approximations of the step-AOA response [Eq. (9)] at Mach numbers 0.5 and 0.7. The simulated and closed-form responses follow each other closely at the low Mach numbers and also at the higher Mach numbers at small s values. They deviate from each other at the steady-state part of the higher, compressible Mach numbers. This deviation is due to the fact that the closed-form response was derived for a flat plate, based on the linearized potential equations, and thus does not hold true for finite-thickness airfoils. The flow on the thin 4% airfoil is characterized by large leading-edge suction and large flow velocities at the leading-edge area. These local flow disturbances are not small, and therefore similarity rules are not applicable, and the flat-plate approximation is no longer valid. The CFD tool has the advantage that it captures well both the unsteady and steady parts of the response.

At Mach 0.7 the flow on the thick, 12% thickness airfoil is dominated by a shock wave, and thus the indicial CFD response and the closed-form response are no longer comparable. In principal, the closed-form functions are not valid in the transonic regime, whereas CFD responses can be calculated throughout this flow range. In practice, the flow analysis of this study is an Euler analysis that does not have the numerical mechanisms to accurately capture the exact location of the shock, and account for flow separation behind it. Thus the computed lift value may be somewhat overestimated.

The incompressible flow theory predicts an up- and down-going Dirac-type behavior of the noncirculatory part of the lift at $s = 0$ (not shown in Fig. 2). The CFD response, which does not distinguish between the circulatory and noncirculatory parts of the lift, predicts this impulsive lift for small s values. The CFD-computed impulsive lift is, however, finite, and is spread on small s values. This is due to numerical factors, and due to the fact that the flow is not completely incompressible at the analyses Mach numbers of 0.11 and 0.2. At the higher Mach numbers (Figs. 2c and 2d), the impulsive part or the CFD-computed response slightly deviates from the closed-form function. The impulsive part of the response quickly decays, according to theory as a function of $1/\sqrt{s}$ [16], and the computed and analytical functions closely follow each other (for small s values).

Next the response to a sharp-edge gust is computed. At each time step, vertical velocities are assigned to grids with flow-direction coordinate $\bar{x}$ of $\bar{x} \leq -1 + s$. At time-step zero the gust front is at the leading edge of the airfoil as depicted in Fig. 1. Figure 3 presents comparison of the CFD-computed gust response and the closed-form approximations, at Mach numbers 0.11 to 0.7, showing a good match between the two, except for the steady-state part at the high Mach numbers, as was the case with the step-AOA response. The results of Figs. 2 and 3 demonstrate that the CFD tool, via the introduced field velocities, can accurately evaluate the indicial AOA and sharp-edge gust unsteady responses, and offer a steady-state response that cannot be accurately calculated by the semi-analytical closed-form approximations.

Lift oscillations are observed at Mach 0.11 for small s values ($0 < s < 2$), when the gust front is on the airfoil, traveling between the leading edge and the trailing edge. These oscillations are suspected to be the result of the convergence process as the gust travels between two consecutive grid points. They are insignificant when the sharp-edge gust response is used in convolution, as demonstrated in the Response to an Arbitrary-Shaped Gust Input section.

A significant advantage of the use of a CFD code for gust response is that a picture of the pressure field on the upper and lower surfaces of the airfoil is readily available at each instant in time. Figure 4 presents snapshots of the pressure field throughout the response to a step AOA. This simulation, and the rest presented in this paper, are of the NACA0012 airfoil. Figure 4a captures the impulsive response right after the step AOA was commanded. The large increase in pressure on the lower surface and large decrease in pressure on the upper surface are responsible for the noncirculatory part of the lift, the large peak in the lift coefficient observed in Fig. 2 for small values of s. After a short time, the impulsive response decays (Figs. 4b–4d), and the lift coefficient rises to its steady-state value (Figs. 4e and 4f).

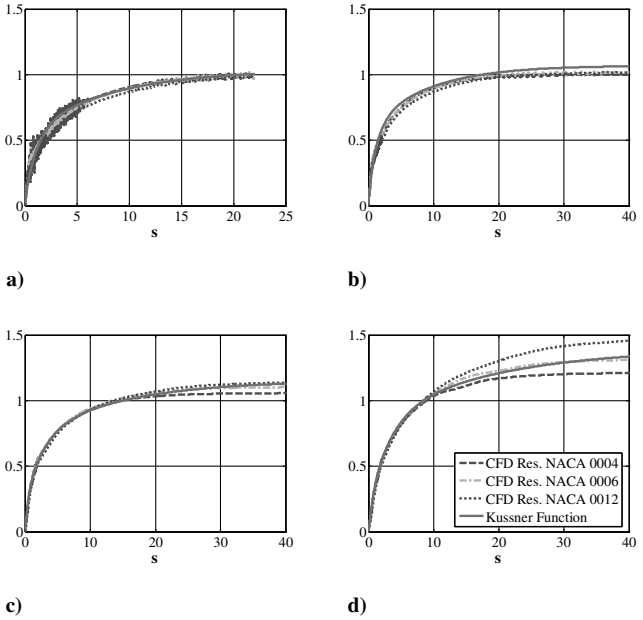

Fig. 3 Normalized indicial response to a sharp-edge gust Mach 0.11 a), Mach 0.2 b), Mach 0.5 c), Mach 0.7 d).

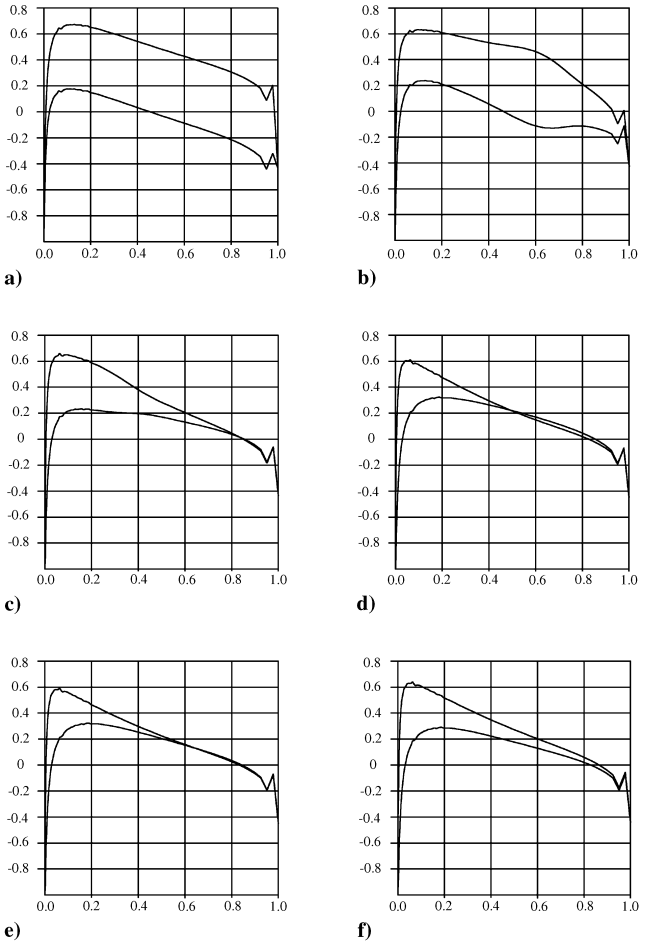

Fig. 4 Snapshots of upper- and lower-surface pressure coefficients in response to a step AOA at times: $s = 0$ a), $s = 0.1$ b), $s = 0.2$ c), $s = 0.3$ d), $s = 0.4$ e), $s = 1$ f); Mach 0.2, 2 deg AOA.

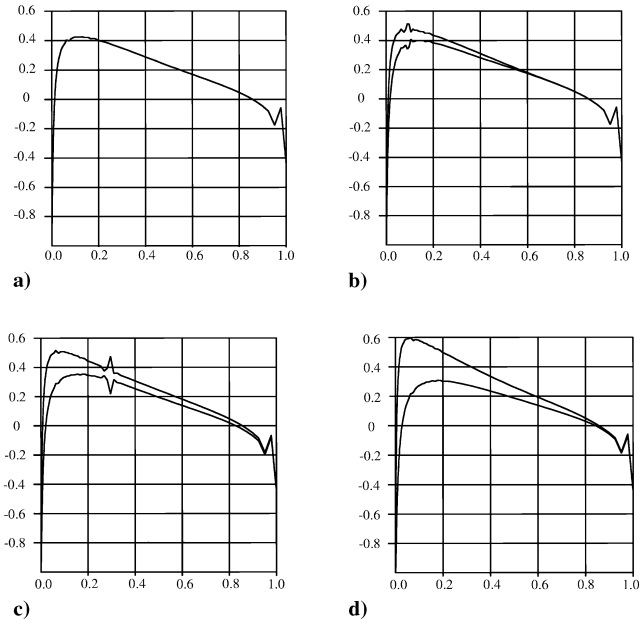

Fig. 5 Snapshots of upper- and lower-surface pressure coefficients at various gust front locations: leading edge a), 10% chord b), 30% chord c), trailing edge d); Mach 0.2, 2 deg AOA.

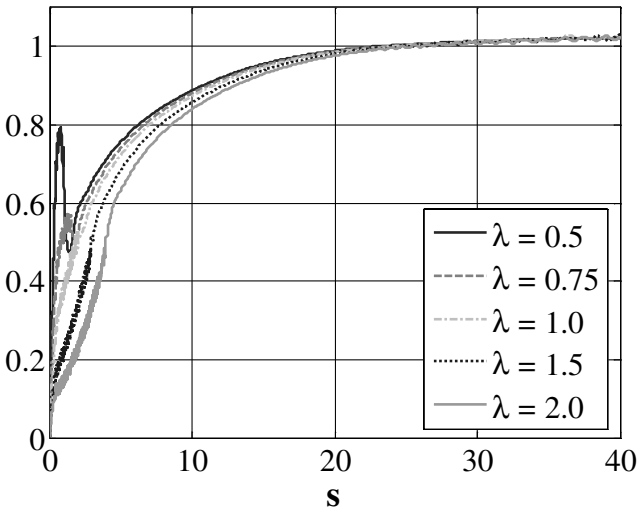

Fig. 6 Response to moving gust, Mach 0.2, 2 deg AOA.

Figure 5 presents snapshots of upper- and lower-surface pressure coefficients in response to a sharp-edge gust, as the gust front travels from the leading to the trailing edge. The location of the gust front is seen clearly in plots 5b and 5c. Figure 5b presents a snapshot of the pressure coefficients at $s = 0.1$. At this time the gust front is located at 0.1 of the chord but the information on the gust perturbation, which travels at the speed of sound, reaches the midchord. Indeed it is seen in Fig. 5b that half the chord generates lift (through pressure difference between the upper and lower surfaces). The zigzag pressure observed at the trailing edge in Figs. 4 and 5 is a nonphysical behavior. It is a known bug of *C* meshes at inviscid Euler analyses, due to the enforcement of the Kutta condition at the trailing edge, and has no influence on the flow analysis or the studied phenomena.

Gust responses were also computed for the case of a traveling gust, in which the gust front is not stationary but rather advances toward or away from the airfoil. Following the terminology of [6] an advance ratio λ is defined as the ratio between the incoming flow Mach number and the Mach number of the relative velocity between the airfoil and the gust,

$$\lambda = \frac{M}{M + U_g/a} \tag{16}$$

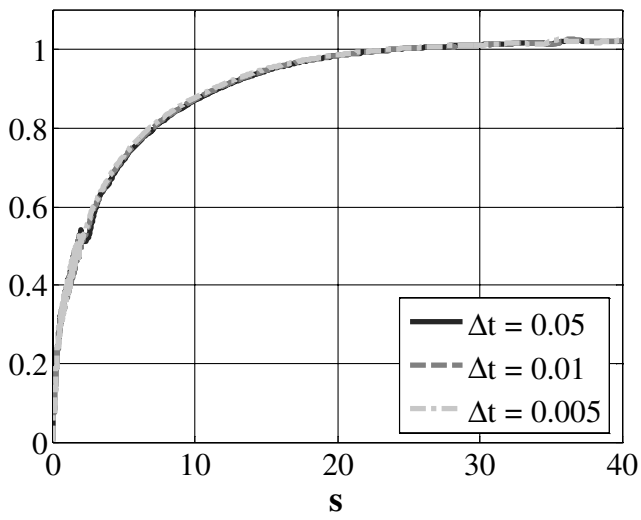

Fig. 7 Normalized sharp-edge gust response using various time steps; Mach 0.2, 2 deg AOA.

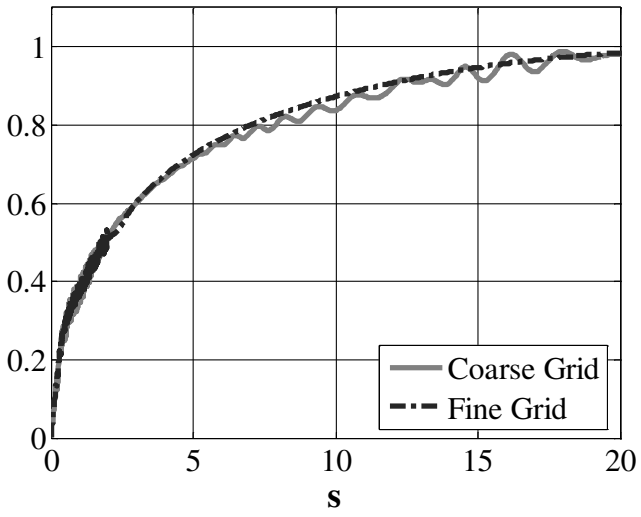

Fig. 8 Normalized indicial response to a sharp-edge gust using fine and coarse grids; Mach 0.2, 2 deg AOA.

In Eq. (16) U_g is the gust forward velocity, and a is the speed of sound. An advance ratio of 1 corresponds to a stationary gust, whereas a step-AOA input is represented by λ values approaching zero. Responses to moving gust with various advance ratio values are plotted in Fig. 6. The simulated response matches the analytical response presented by Miles [17].

Parametric Study on the Effect of Grid Density and Time-Step Size on the Response

Gust responses were computed with various time steps and various grid densities. Figure 7 presents time histories of responses using nondimensional time steps of 0.05, 0.01, and 0.005. From Fig. 7 it is seen that within this range of acceptable time steps (acceptable in the sense that they all satisfy the CFL stability condition but are not extremely small) the selection of time step has no effect on the gust response. Figure 8 presents a comparison of sharp-edge gust responses computed with the former grid, and a coarser grid of 159 grid points in the chordwise direction, and 44 grid points in the normal direction. The coarse grid resulted in lift oscillations at large values of s. Lift oscillations are also observed for $0 < s < 2$, when the gust front travels over the airfoil. The same oscillations were reported in [6], where they are attributed to the curvilinear nature of the grid, which results in a nonstraight gust front. However, whereas [6] notes that these oscillations are

independent of the grid size, here it is noted that the oscillations' amplitudes were smaller when using the finer grid. It is speculated that these oscillations result from the convergence process of the numerical scheme as the gust front travels between two consecutive grid points. These fluctuations have an insignificant effect when the sharp-edge gust response is used in a convolution scheme to predict responses to arbitrarily shaped gust inputs. Finally, gust responses were computed for meshes with different wake lengths, shown in Fig. 9. A typical wake size of about six chords was found to be sufficient for accurately capturing gust responses.

Response to an Arbitrary-Shaped Gust Input

The CFD-computed sharp-edge gust responses were used in convolution to predict the responses to a one-cycle sinusoidal and to one-minus-cosine gust inputs of various wavelengths. These responses were also computed by direct simulation in a CFD run and by convolution with the closed-form function. Figure 10 presents the various responses. The good fit between the direct simulation and the responses by convolution validates the newly introduced capability of the CFD code to simulate gust responses, and the adequacy of the CFD-based sharp-edge gust response to serve as a ROM for predicting responses to arbitrary gust inputs. The use of convolution presents a significant time savings compared to the full CFD simulation, as one sharp-edge gust response can serve to predict responses to as many inputs as desired. In the current case, the sharp-edge gust response was simulated over 10 K iterations, which required 2 h to run on a 12-processor of type R10000 on an Origin SGI workstation. The convolution is performed in a few seconds. The one-minus-cosine and one-cycle-sinusoidal responses of Fig. 10 were simulated over 50 K iterations each, or about 10 h run time.

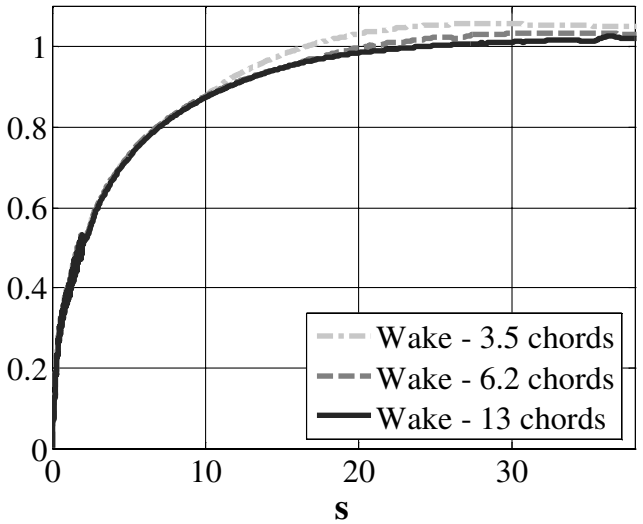

Fig. 9 Normalized indicial response to a sharp-edge gust using grids with different wake lengths; Mach 0.2, 2 deg AOA.

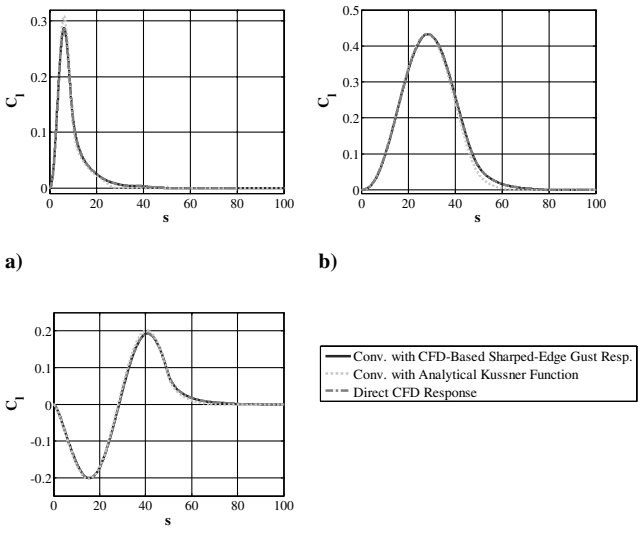

Fig. 10 Comparison of lift responses to a a) one-minus-cosine gust of 5 chords, b) one-minus-cosine gust of 25 chords, c) sinusoidal gust of 25 chords; Mach 0.2, 2 deg AOA.

ARMA Model

ARMA coefficients for a 2,1 ARMA model of the form of Eq. (11) were identified from CFD responses to random gust excitation. The input gust signal, that is the vector of time-dependent gust vertical velocities *at the leading edge*, is a filtered random time series with Gaussian distribution. Filtering was applied to control the range of excited frequencies, such that any frequency spectrum of interest can be excited.

The current study focuses on responses of the system to one-minus-cosine shaped gusts of wavelengths ranging from 5 to 25 chords. Thus the range of frequencies of interest is between $1/5$ to $1/25$ cycles per chord, which at Mach 0.2 corresponds to $0.2/5$ and $0.2/25$ cycles per nondimensional time unit. Filtering was applied such that the input signal excites frequencies at about this range.

Because the excitation is applied to the CFD system, which by itself is a discrete-time system, the intervals at which the excitation is applied and the system is sampled, correspond to the CFD time step Δs. The sampling rate is therefore $f_s = 1/\Delta s$, from which signals of frequencies of up to half the sampling rate, denoted by f_{Nyq}, can be reconstructed (based on the Nyquist Theorem, see Chapter 13.7, pp. 444–445 of [18]). Since in CFD analyses the typical time steps are very small, the maximum frequency that can be identified is high and exceeds the frequency range of interest. In the current study CFD time steps of 0.01, 0.02, and 0.04 were used. These values were chosen according to the observations on the effect of the time step reported in the Parametric Study on the Effect of Grid Density and Time-Step Size on the Response section. Within this range, the choice of time step had no impact on the response, that is, responses based on all three time steps were basically as good for parameter identification. The frequency resolution of a length-N data set, given by f_{Nyq}/N, should be adequate for the representation of the lowest frequencies of interest. Therefore, the sampling interval and the length of the sampled signal (the number of samples) need to be

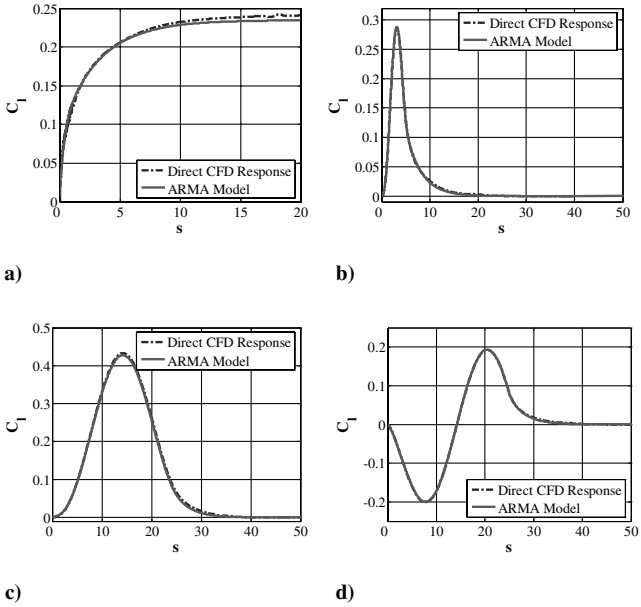

Fig. 11 ARMA model lift responses to a sharp-edge gust a), one-minus-cosine gust of 5 chords b), one-minus-cosine gust of 25 chords c), sinusoidal gust d); Mach 0.2, 2 deg AOA.

Table 1 Fit parameter for various identification and validation signals

Time step	Signal length	η, %			
		Sharp-edge gust	$1-\cos(\frac{2\pi}{5}\bar{x})$	$1-\cos(\frac{2\pi}{25}\bar{x})$	$1-\sin(\frac{2\pi}{25}\bar{x})$
0.01	2,400	62	91	88	91
0.01	10,000	91	95	97	96
0.01	15,000	80	97	95	97
0.02	2,700	88	96	96	97
0.02	4,100	69	80	75	80
0.02	5,400	90	98	97	99
0.04	2,800	60	87	80	87
0.04	5,400	71	78	78	75

adjusted to fit the desired frequency range and resolution.

2, 1 ARMA model coefficients were identified using the Matlab® System Identification Toolbox [19]. These models were used to predict the responses to a sharp-edge, a one-cycle sinusoidal, and to one-minus-cosine of 5 and 25 chord-lengths gust inputs. Figure 11 presents a comparison of responses based on an ARMA model and direct CFD simulation, where it can be seen that the ARMA model captures the response very accurately. The parameters of the ARMA model of Fig. 11 were extracted from an identification data set that consists of the CFD response to a random gust input that was filtered for a frequency range of 0.005 to 0.05 cycles per nondimensional seconds. The identification data were computed with a CFD time step of 0.02 for about 5000 iterations. ARMA models were also identified based on other identification data (random input strings of various time step and length) and yielded similar results. Table 1 presents fit parameters corresponding to various identification and validation signals. It is observed that the models predict the one-minus-cosine and one-cycle-sinusoidal responses better than they do the sharp-edge gust response. This is due to the fact that the identification data were intentionally focused on a limited range of frequencies.

The significant advantage of the ARMA model over the direct CFD simulation is that it only requires one, relatively short, CFD analysis for the generation of the identification data, and then responses to all input signals can be computed in a fraction of a second. For example, the responses of Fig. 11 were computed by an ARMA model identified from 5 K CFD iterations (1 h run time), and by four direct CFD simulations at a total of 42.5 K iterations (over 8 h run time). The time required for ARMA model identification is on the order of seconds and is negligible compared to generation of the identification data. The iterations and time saving would be much more pronounced in the environment of aircraft design, in which many responses have to be computed, and where each run is of a complete aircraft configuration and thus of significantly larger run time per iteration.

Finally, we examine the use of ARMA models for the prediction of gust responses in the transonic flow regime. At Mach 0.7, zero AOA, the steady flow is linear. However, as the one-minus-cosine gust travels along the chord, the gust-induced AOA is increased and a strong shock is developed. Figure 12 presents snapshots of upper- and lower-surface pressure coefficient as a one-minus-cosine gust with an amplitude equivalent to 10 deg AOA travels along the chord. The Euler flow analysis presents the strong shock that develops, but it does not capture flow separation that most likely exists in this flow.

Figures 13 and 14 present time histories of the lift- and pitching-moment coefficients in response to one-minus-cosine gust inputs of

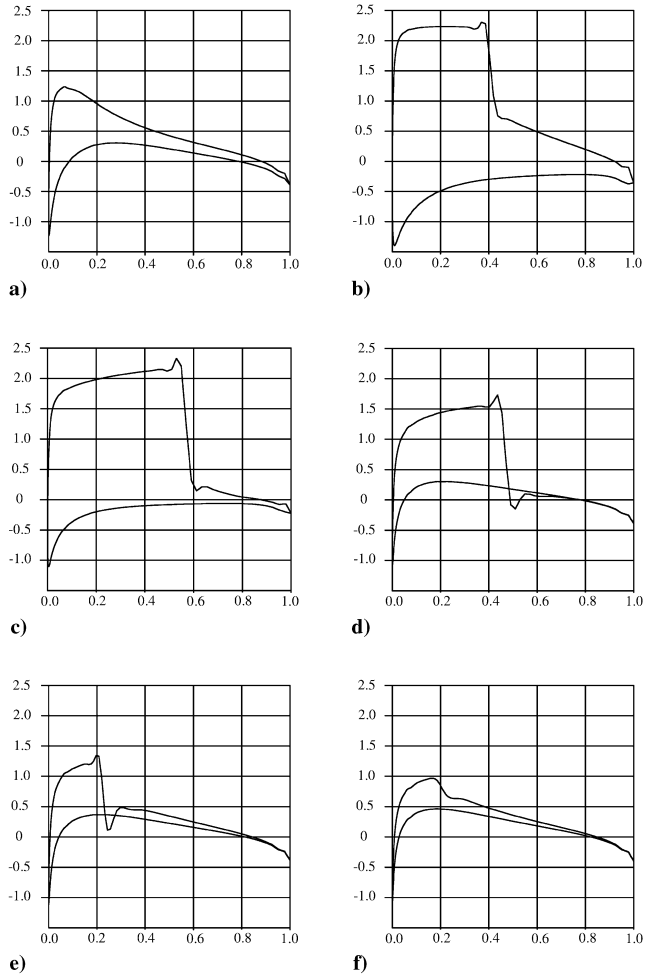

Fig. 12 Snapshots of upper- and lower-surface pressure coefficients in response to a one-minus-cosine gust of 5 chords at times $s = 1.4$ a), $s = 2.8$ b), $s = 4.2$ c), $s = 7$ d), $s = 9.8$ e), $s = 12.6$ f); Mach 0.7, 10 deg AOA.

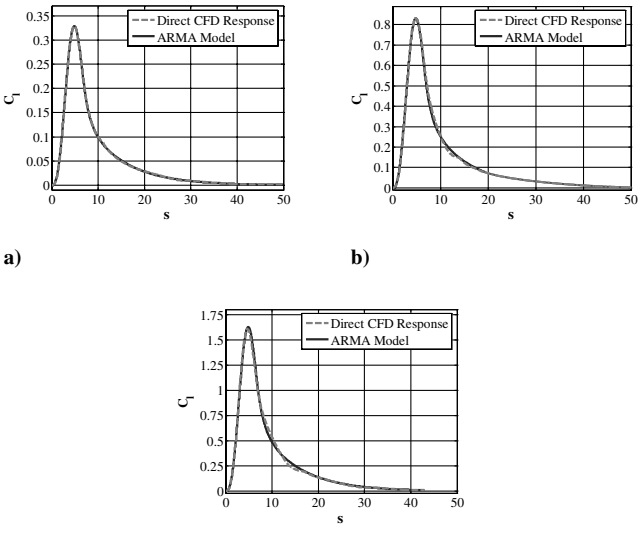

Fig. 13 ARMA model lift responses to a one-minus-cosine gust of 5 chords and 2 deg AOA a), 5 deg AOA b), and 10 deg AOA c); Mach 0.7.

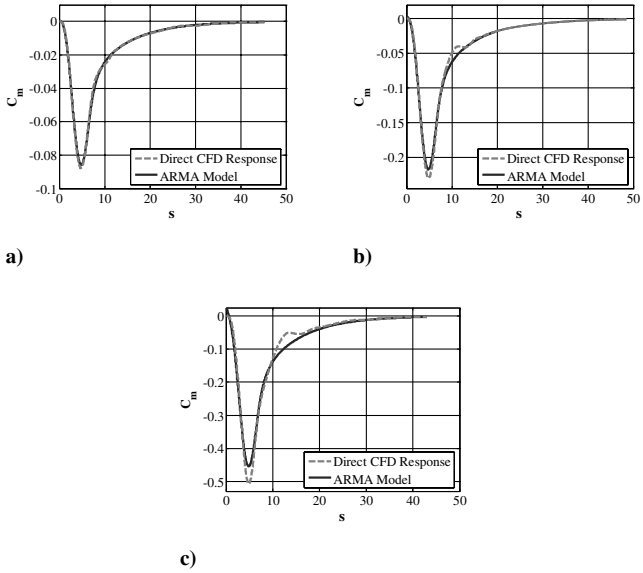

Fig. 14 ARMA model pitching moment responses to a one-minus-cosine gust of 5 chords and 2 deg AOA a), 5 deg AOA b), and 10 deg AOA c); Mach 0.7.

Table 2 Parameter for lift and pitching moment response ARMA models; Mach 0.7.

	η, %		
	2 deg AOA	5 deg AOA	10 deg AOA
Lift response	99	95	95
Pitching moment response	96	90	87

amplitudes equivalent to 2, 5, and 10 deg AOA. The responses of Figs. 13 and 14 were computed by direct CFD simulation and from an ARMA model. The latter was identified based on data from one flow simulation, the response to random gust excitation of amplitude of 2 deg AOA, at Mach 0.7. Because the Euler analysis does not predict flow separation, the CFD-computed lift is linear with respect to the angle of attack, and is thus predicted very accurately by the linear ARMA model, as seen in Fig. 13 and from the fit parameters of Table 2. For a more realistic flow analysis at these flow conditions, and to test how well the linear ARMA model can predict the lift history in real nonlinear conditions, a viscous Navier–Stokes analysis should be attempted. The pitching moment, on the other hand, is a nonlinear function of the AOA, even in an inviscid Euler analysis. This is due to the aft movement of the center of pressure in the vicinity of the shock wave. It is seen in Fig. 14, and from the fit parameters of Table 2, that the prediction capability of the linear ARMA model slightly degrades at large AOAs. It is interesting to note that the pitching moment buildup and decay in time is captured accurately, and that it is only the amplitude that the linear model does not capture completely.

The results of Figs. 13 and 14, and Table 2 demonstrate that the ARMA model is a very useful tool for computing tuned-gust responses. The model is constructed based on a single CFD simulation, and can then be used to rapidly and accurately compute responses to arbitrary gust excitations, even in the transonic flow range. The ARMA model can be used to identify critical loading cases, which can then be simulated with a full CFD run. The combination of a rapid reduced-order model and full CFD simulation offers a computationally efficient and accurate tool set for analyzing gust responses.

Summary

Two approaches for the computation of gust responses were presented based on direct CFD simulation and on reduced-order modeling. The EZNSS CFD code was enhanced to simulate responses to arbitrary gust excitations. Responses to step-AOA and sharp-edge gust inputs were computed for the NACA0004, NACA0006, and NACA0012 airfoils, for various Mach numbers. Validation was achieved by comparison of the responses to the closed-form approximations, which indicated that the CFD simulations capture accurately the unsteady part of the response, for small times, and offer a steady-state response that is valid for finite-thickness airfoils. Responses to various gust inputs were simulated by the CFD code and computed via convolution with a CFD-based sharp-edge gust response, and were found to be in very good fit. The use of convolution offers a great deal of computational savings compared to the full direct CFD simulation. Only one CFD simulation of the sharp-edge gust response is required, from which responses to arbitrary gust profiles can be calculated quickly and accurately by convolution.

Parametric ARMA ROMs for gust response were identified at various Mach numbers. The ARMA model is a compact time-domain model of the aerodynamic response that can be used for rapid gust simulations, and for ASE applications. It is easy to identify and offers a significant computational savings compared to the full CFD simulation. It was shown that, for the test cases studied, at the linear flow regime the ARMA model captured the gust response perfectly. At the nonlinear transonic regime the linear ARMA model still captured the response's nature, but the amplitudes were slightly less accurate. The analyses of the current study were all inviscid, so conclusions cannot be drawn on the model performance in detached flows. The combination of ARMA modeling and full CFD simulation offers a powerful and computationally efficient set of tools for predicting tuned-gust responses. The ARMA model can be used to rapidly point out to critical loading cases, which can then be studied with a full CFD simulation, with the benefits of a full picture of pressure distribution throughout the gust penetration. A current study by the authors extends the CFD response and reduced-order modeling to finite wings, rigid and elastic.

Acknowledgement

The authors wish to thank P. C. Chen of Zona Technologies for his continuous encouragement to study CFD-based gust response and for his useful advice throughout this study.

References

[1] Karpel, M., Moulin, B., and Chen, P. C., "Dynamic Response of Aeroservoelastic Systems to Gust Excitation," *Journal of Aircraft*, Vol. 42, No. 5, Sept.–Oct. 2005, pp. 1264–1272.

[2] Karpel, M., Moulin, B., Anguita, L., Maderuelo, C., and Climent, H., "Aeroservoelastic Gust Response Analysis for the Design of Transport Aircrafts," *Proceedings of the 45th AIAA/ASME/ASCE/AHS/ASC Structures, Structural Dynamics and Materials Conference*, AIAA, Reston, VA, 2004.

[3] Gennaretti, M., and Mastroddi, F., "Study of Reduced-Order Models for Gust-Response Analysis of Flexible Wings," *Journal of Aircraft*, Vol. 41, No. 2, March–April 2004, pp. 304–313.

[4] Parameswaran, V., and Baeder, J. D., "Indicial Aerodynamics in Compressible Flow—Direct Computational Fluid Dynamics Calculations," *Journal of Aircraft*, Vol. 34, No. 1, Jan.–Feb. 1997, pp. 131–133.

[5] Singh, R., and Baeder J. D., "Direct Calculation of Three-Dimensional Indicial Lift Response Using Computational Fluid Dynamics," *Journal of Aircraft*, Vol. 34, No. 4, July–Aug. 1997, pp. 465–471.

[6] Singh, R., and Baeder, J. D., "Generalized Moving Gust Response Using CFD with Application to Airfoil-Vortex Interaction," AIAA Paper 97-2208, 1997.

[7] Yang, G., and Obayashi, S., "Numerical Analyses of Discrete Gust Response for an Aircraft," *Journal of Aircraft*, Vol. 41, No. 6, 2004, pp. 1353–1359.

[8] Levy Y., "Numerical Simulation of Dynamically Deforming Aircraft Configurations using Overset Grids," *Journal of Aircraft*, Vol. 38, No. 2, 2001, pp. 349–354.

[9] Bisplinghoff, R. L., Ashley, H., and Halfman, R. L., *Aeroelsticity*, Dover, New York, 1996.

[10] Mazelsky, B., and Drischler, J. A., "Numerical Determination of

Indicial Lift and Moment Functions for a Two-Dimensional Sinking and Pitching Airfoil at Mach Numbers 0.5 and 0.6," NACA TN 2793, 1952.

[11] Lomax, H., "Indicial Aerodynamics," *AGARD Manual of Aeroelasticity, Pt. II*, Nov. 1960, Chap. 6.

[12] Leishman, J. G., "Indicial Lift Approximations for Two-Dimensional Subsonic Flow as Obtained from Oscillatory Measurements," *Journal of Aircraft*, Vol. 30, No. 3, 1993, pp. 340–351.

[13] Leishman, J. G., "Validation of Approximate Indicial Aerodynamic Functions for Two-Dimensional Subsonic Flow," *Journal of Aircraft*, Vol. 25, No. 10, Oct. 1988, pp. 914–922.

[14] Levy, Y., "Numerical Analysis of Three-Dimensional Flow Solvers Applied to High Angle-of-Attack Flows," Ph.D. Thesis, Stanford University, 1994.

[15] Raveh, D. E., "Identification of Computational-Fluid-Dynamics Based Unsteady Aerodynamic Models for Aeroelastic Analysis," *Journal of Aircraft*, Vol. 41, No. 3, May–June 2004, pp. 620–632.

[16] Iosilevskii, G., and Yariv, E., "Tab Control and History-Dependant Forces," Technion—Israel Institute of Technology TAE Rept. 891, July 2002.

[17] Miles, J. W., "The Aerodynamic Force on an Airfoil in a Moving Gust," *Journal of Aerospace Sciences*, Nov. 1956, pp. 1044–1050.

[18] Ljung, L., *System Identification, Theory for the User*, 2nd ed., Prentice–Hall, Upper Saddle River, NJ, 1999.

[19] Matlab System Identification Toolbox User's Guide, Ver. 5.0, The MathWorks, Inc., Natick, MA, April 2001.

C. Pierre
Associate Editor